WIND ENERGY
Wind Energ. 2010; **00**:1–29
DOI: 10.1002/we

RESEARCH ARTICLE

Implementation of a nonlinear foundation model for soil-structure interaction analysis of offshore wind turbines in FAST

V. L. Krathe[1] and A. M. Kaynia[2,3]

[1]DNV GL AS, Oslo Norway
[2]Norwegian University of Science and Technology, Trondheim, Norway
[3]Norwegian Geotechnical Institute, Oslo, Norway

ABSTRACT

Bottom-fixed *offshore wind turbines* (OWTs) involve a wide range of engineering fields. Of these, modelling of foundation flexibility has been given little priority. This paper investigates the modelling of bottom-fixed offshore wind turbines in the nonlinear aero-hydro-servo-elastic simulation tool *FAST v7*. The OWT considered is supported on a monopile. The objective of this paper was to implement a nonlinear foundation model in this software. The *National Renewable Energy Laboratory*'s (NREL) idealized 5MW reference turbine was used as a base for the analyses.
Default modelling of foundation in FAST v7 is by means of a rigid foundation. This implies that soil stiffness and damping is disregarded. Damping may lead to lower design loads. A softer foundation, on the other hand, will increase the natural periods of the system, shifting them closer to the frequencies of the environmental loads. This may in turn lead to amplified moments at the mudline. Therefore, it is important to include soil stiffness and damping in analyses.
In this paper, a nonlinear foundation model is introduced in FAST v7 by means of uncoupled parallel springs. To verify that the implementation is successful, nonlinear load-displacement curves of the foundation spring are presented. These show the typical hysteresis loops of an inelastic material, which confirms the implementation.

KEYWORDS

wind turbine; nonlinear foundation; monopile; FAST; modelling

Correspondence

Veronica Liverud Krathe, DNV GL AS, Veritasveien 1, 1363 Høvik, Norway. E-mail: veronica.krathe@dnvgl.com

Received . . .

1. INTRODUCTION

The wind energy industry has developed and grown remarkably during the recent years. Being renewable and vastly spread across the planet, it is an important contribution to the world's increasing need for energy, and to environmental issues. Since winds are stronger and more stable at sea than onshore, there has been an increased focus on installing wind turbines offshore. In the 1990s, the world's first offshore wind turbine farm, *Vindeby*, was built in Denmark. The offshore wind turbine industry has increased significantly since then. About 90% of the world's *offshore wind turbines* OWTs are installed

Prepared using weauth.cls [Version: 2010/06/17 v1.00]

in Europe, with the UK as the leading country [1]. Correspondingly, the depths at which OWTs have been installed are also increasing. This leads to larger environmental loads, which again calls for stronger, more advanced support structures. Still, roughly 80% of offshore wind turbines in Europe are supported by the traditional monopile substructures [2]. One reason for the preference for monopiles is their simplicity of installation [3].

Harnessing wind energy covers a wide range of engineering fields, from aerodynamics and structural dynamics to electrical generators and grid networks. Historically, modelling of foundation flexibility related to wind turbines has come in the shadow of other, more visible aspects, such as aerodynamic efficiency, electricity generation, structural dynamics, and hydrodynamics. However, the accuracy of a wind turbine simulation depends on, among other factors, how realistically the modeled foundation represents the true soil-structure interaction. Currently, most wind turbine modelling tools are quite advanced in computing aerodynamic and hydrodynamic loads, while soil-structure interactions are only considered in a very simplified manner. According to [4], soil-pile interaction modelling for piled foundations is one of the most critical aspects regarding modelling of OWT substructures. In general, there is a lack of simplified foundation models that provide sufficient accuracy for detailed design of monopiles. The absence of appropriate representations may lead to under-predicted or over-predicted fatigue loads.

The purpose of this paper is to expand the modelling of soil-structure interaction of bottom-fixed wind turbines by introducing a nonlinear foundation representation in an existing software. Specifically, the aero-hydro-servo-elastic simulation tool *FAST v7* is modified for this purpose. The *NREL* (National Renewable Energy Laboratory) has developed an idealized 5MW reference wind turbine [5], including input files appropriate for FAST v7 that contains its properties. This reference turbine will be used as a base model in the following, and will later be addressed as *NREL 5MW*. A nonlinear foundation is modeled in FAST by means of parallel elastic perfectly-plastic springs as originally proposed by [6].This model can be attached to the tower base at mudline.

1.1. Soil Damping

As a consequence of installation in deeper waters, OWT tower heights and blade lengths have increased. This moves the dynamic response of the wind turbine structure into a range of frequencies that is closer to those of wind and waves, and closer to the operating frequency. Therefore consideration of damping is important to prevent large oscillation amplitudes [7].

Bottom-fixed OWTs experience damping in different forms. The main types of damping are aerodynamic damping, soil damping, hydrodynamic damping and structural damping, in addition to dampers installed in the tower. Of these, the largest contributor is aerodynamic damping. During standstill, or when the wind turbine is idling, the aeroelastic damping becomes insignificant and the other types of damping play a larger role. Next to aerodynamic damping, soil damping gives the largest contribution to overall damping [8]. Soil damping results in energy dissipation and alters the cyclic response of the structure. The investigation of this influence on the structural response of OWTs is scarce [9].

Soil damping mainly exists in two types, namely *radiation damping* and *hysteretic damping*. The former concerns dissipation of energy through radiation of waves generated by the foundation's oscillation, whereas the latter represents energy loss due to inelastic behavior of the soil. Radiation damping may be neglected for frequencies typically below 1 Hz [10]. Since the operating frequencies and the first natural frequencies of the tower, and the environmental load frequencies normally lie below this frequency [3], radiation damping is normally small. Therefore, this study will only examine the hysteretic damping. When a structure or foundation with hysteretic damping is subjected to cyclic loading, the load-displacement curve forms a hysteresis loop. The energy dissipated during one deformation cycle is directly related to the area under the hysteretic loop. Damping has also an important impact on the fatigue life of OWTs, dominated by a large number of small-amplitude cyclic movements.

Therefore, by representing the force-displacement (or moment-rotation) response of the foundation by a nonlinear relationship, damping is automatically incorporated in the foundation. Foundation damping may lead to lower design load estimates. A softer foundation, on the other hand, will increase the natural periods of the system, shifting them closer to the frequencies of the environmental loads. This may in turn lead to amplified overturning moments at the mudline. In

Wind Energ. 2010; **00**:1–29 © 2010 John Wiley & Sons, Ltd.
DOI: 10.1002/we
Prepared using weauth.cls

addition to damping, a nonlinear force-displacement will correctly capture the varition of stiffness with load level which is again important for correct modelling of the foundation.

1.2. Monopile models

The loads on the structure are resisted by lateral soil pressure on pile foundation [11]. FEM-modelling of the soil as a continuum is the most realistic way to describe the soil-pile system, but these models are time consuming for OWT analyses [4]. There exists other more rigorous models. One example is [12]. Here, both an approximate analytical solution for piles, which was originally developed by [13], and a Green's-Functions-based impedance matrix for a slab foundation a semi-analytical solution [14], were used. Another advanced solution for pile foundation is the visco-elastodynamic model PILES developed by [15], [16]. The computational tool in PILES is based on the analytical solution of wave propagation in layered soil media considering equilibrium of stresses and imposition of compatibility of displacements at the pile-soil interface. The model is formulated in the frequency domain and has the advantage of computing radiation damping due to pile vibration. Another advantage of this model (and other elasto-dynamic codes) is that it directly uses the shear wave velocities of the layers which are directly measureable in situ by a variety of geophysical methods. Therefore, one could avoid empirical relationships for estimation of the soil modulus as in conventional Winkler models. Results of this model are presented later in this paper.

[17] consider three alternative methods for modelling of foundation for OWTs in shallow-water. The simplest model considered is a fixed-base model, not considering the soil profile at turbine site. The other two models both account for flexibility related to soil properties. One of them is an apparent fixity (AF) model, the other a distributed springs (DS) model. The AF model includes a rigid connection located at a certain depth that provide appropriate stiffness of the soil-pile interaction. The DS model, on the other hand, uses the real length of the monopile with attached distributed linear elastic springs to represent the soil. This model is a simplification of the traditional p-y curves used in offshore pile design (see [18] for a detailed list of references and summary of equations). The last two representations are based on the analyses of [19], and also presented in [20]. [17] conclude that, for long-term considerations, the two flexible foundation models (the AF and the DS model) show larger extreme loads than the model with a fixed base. The dynamics of the turbine is highly affected by the flexibility of the foundation model, as the lowered stiffness of the system gives less high-frequency content in the response, higher RMS levels of response, and larger long-term loads [17].

A recent model for a cyclic pile-soil interaction was developed by [21], and [22]. This model includes hysteretic damping from the soil. It also considers gaps that occur between pile and soil when loading is reversed. The soil model is based on a Winkler model [8] in which the pile is modeled using a beam, and the soil is represented by uncoupled nonlinear springs. [8] has implemented this 2D model in the aeroelastic code Flex5 for analysis of monopile-supported OWT. The model is further developed by [23], being extended to 3D. The complete result was also presented by [24].

A model where the monopile ends at the mudline, with attached lateral rocking and translational springs at the bottom, is a simpler way of modelling the foundation response. The springs may be *coupled* or *uncoupled*, *linear* or *nonlinear*. While coupled springs is more realistic then uncoupled springs, they provide a stiffness matrix with off-diagonal terms. A coupled stiffness matrix will in general make calculations more complicated. However, one can avoid the off-diagonal terms by addition of a *rigid link* [25] at the base of the pile and placing uncoupled translational and rocking springs here. A presentation of the rigid link method is given in [26].

[25] have applied such a procedure for analysis of an OWT. To obtain a nonlinear, load-dependent formulation of these, the magnitudes of the damping and stiffness were iteratively updated as a function of mudline pile loads using a separate geotechnical program.

Modelling the flexibility of the foundation is a shortcoming in most softwares for simulations of OWTs today [4]. Simplified, but accurate models are highly needed for more realistic analysis of OWTs.

Table I. Properties of the NREL 5 MW Baseline OWT with a monopile support structure [5].

Rating	5 MW
Rotor orientation, configuration	Upwind, 3 blades
Rotor diameter	126 m
Hub-height	90 m
Tower top diameter, wall thickness	3.87 m, 0.019 m
Tower base diameter, wall thickness	6.0 m, 0.027 m
Substructure diameter, wall thickness	6.0 m, 0.06 m
Cut-in, rated, cut-out wind speed	3 m/s, 11.4 m/s, 25 m/s
Rated rotor speed	12.1 rpm
Rated tip speed	80 m/s
Rotor mass	110,000 kg
Nacelle mass	240,000 kg
Tower mass	346,460 kg
Mean sea level	20.0 m

2. IMPLEMENTATION OF NONLINEAR FOUNDATION MODEL

Implementation of a nonlinear foundation flexibility in FAST v7 has been achieved in this study by applying nonlinear properties to an uncoupled foundation stiffness matrix at the mudline of the monopile. This leads to a nonlinear relationship between loads and displacements implying that the stiffness of the spring will depend on the load and displacement.

To simplify the study of offshore wind technology, NREL has developed a standard set of turbine specifications for an idealized offshore 5 MW baseline wind turbine supported by a monopile. NREL has implemented a model of this reference turbine in FAST. This model is used as a base for analyses in this paper, and it will subsequently be referred to as the *NREL 5MW*. Properties of the NREL 5MW are given in Section 2.1.

FAST is a time-domain *computer-aided engineering* (CAE) tool for simulating dynamic response of horizontal-axis wind turbines, including both hydrodynamic and aerodynamic loads. It is developed by the United States *Department of Energy's* (DOE's) National Renewable Energy Laboratory, and is an open source software, written in the programming language Fortran. FAST models structural dynamics of the support structure, tower, rotor and nacelle, as well as control and electrical drive dynamics. Both land-based, offshore bottom-fixed and offshore floating wind turbines can be modeled, and they may be two- or three-bladed. FAST does not provide a graphical user interface. All information given to the user and by the user is in the form of text files and scripts.

The latest version of this tool is FAST v8. Currently, however, FAST v8 can only model a bottom-fixed monopile with rigid connections between the substructure and the seabed. FAST v7, on the other hand, provides the possibility of substituting the rigid connection at the bottom of the monopile with linear springs in each dof. Therefore, this version was used in the present study. For monopiles, the advantages of FAST v8 are minor, while FAST v7 has several advantages, e.g. the option of including wave stretching in the hydrodynamic load calculation, which is important in shallow water, and the ability to make easy customizations for soil models [27]. Therefore, when subsequently referring to FAST in this paper, FAST v7 is the version that is meant.

2.1. NREL 5MW OWT

The NREL 5MW is meant to be representative of a large land- or sea-based multimegawatt wind turbine, also appropriate for deep water sites. The choice of a power rating of 5 MW is based on the idea that a cost-efficient deep-water turbine should be rated at least at 5 MW [5]. The properties have been obtained from publicly available information on real wind turbine prototypes and conceptual models. Table I lists some of the parameters of the turbine.

In NREL 5 MW the tower ends at the tower base, 10 m above MSL. From there, the monopile extends down to the mudline at 20 m below MSL. The diameter and wall-thickness of the tower are linearly tapered from the top to the tower base. The monopile has a constant diameter and wall-thickness of 6 m and 0.060 m, respectively [11]. Since the default model in FAST attaches the monopile to the mudline through a rigid connection, the depth of the monopile into the ground

Wind Energ. 2010; **00**:1–29 © 2010 John Wiley & Sons, Ltd.
DOI: 10.1002/we
Prepared using weauth.cls

Table II. First natural frequencies of the tower [5].

Mode	Description	Natural frequency (Hz)
1	1st Tower fore-aft	0.324
2	1st Tower side-to-side	0.312
:	:	:
:	(Blades)	:
12	2nd Tower fore-aft	2.900
13	2nd Tower side-to-side	2.936

is not given. However, in Section 2.2.2 the flexibility of the foundation is modeled based on a monopile penetration depth of 36 m below the mudline [19].

In addition, blade structural and aerodynamic properties, hub and nacelle properties, drivetrain properties, tower properties, and control system properties are given. The turbine utilizes active yaw, continuously orienting the rotor to face the wind.

The full-system natural frequencies of the fore-aft and side-to-side tower mode shapes are given in Table 2.1.

It is important to note that the aforementioned natural frequencies and mode shapes are related to the full system - that is, how the blades couple with the drivetrain and tower. They are obtained using a FAST linearization analysis followed by an eigenvalue analysis. These mode shapes are outputs from FAST, whereas individual mode shapes for tower and blades are input to FAST. A three-bladed HAWT will have operating natural frequencies of 1P and 3P. For the NREL 5MW turbine, with a rated rotor speed of 12.1 rpm, this implies the following system natural frequencies:

$$1P = 0.20Hz \tag{1}$$

$$3P = 0.60Hz \tag{2}$$

Evidently, the wind turbine has a soft-stiff design, since the natural frequency of the first tower mode is larger than 1P but less than 3P.

2.2. Kinematic hardening nonlinear foundation model

An approach for modelling the yielding behavior of materials and structures by means of parallel springs was presented by [6].

By applying several parallel elastic perfectly-plastic springs, one can obtain a smooth and realistic load response to the deflection, see Figure 1. Here, F represents either moment or force, and correspondingly δ may represent rocking or translation.

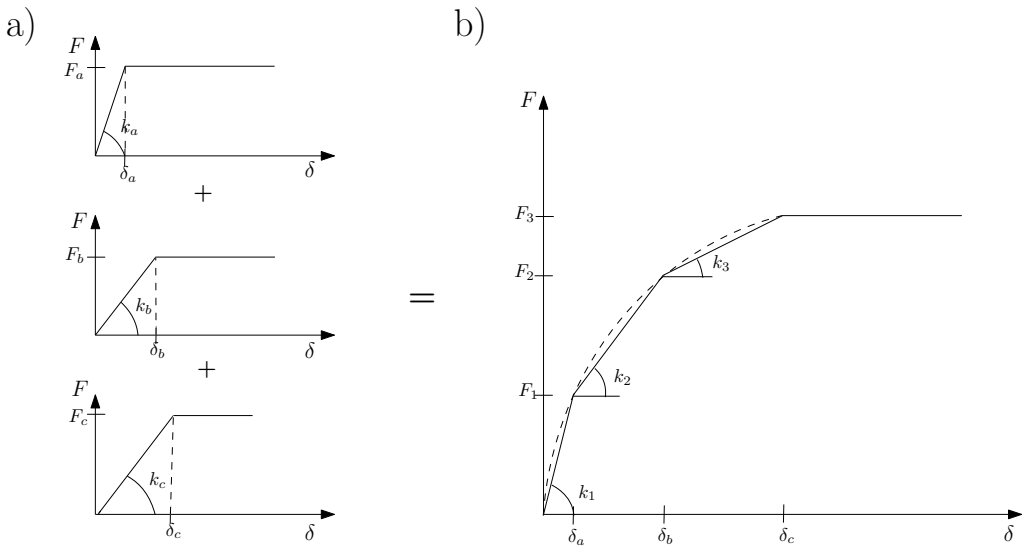

Figure 1. Representation of nonlinear foundation by means of parallel elastic perfectly-plastic springs.

Figure 1 shows schematically how the individual springs can be derived for a case where the force-displacement curve is represented by a piecewise linear variation with three points. For the case in Figure 1, one can write:

$$\begin{aligned} k_1 &= k_a + k_b + k_c \\ k_2 &= k_b + k_c \\ k_3 &= k_c \end{aligned} \tag{3}$$

and

$$\begin{aligned} F_1 &= F_a + k_b\delta_a + k_c\delta_a \\ F_2 &= F_a + F_b + k_c\delta_b \\ F_3 &= F_a + F_b + F_c \end{aligned} \tag{4}$$

from which one can establish the individual springs in Figure 1a).

Figure 2 illustrates the path of unloading according to this model.

Wind Energ. 2010; **00**:1–29 © 2010 John Wiley & Sons, Ltd.
DOI: 10.1002/we
Prepared using weauth.cls

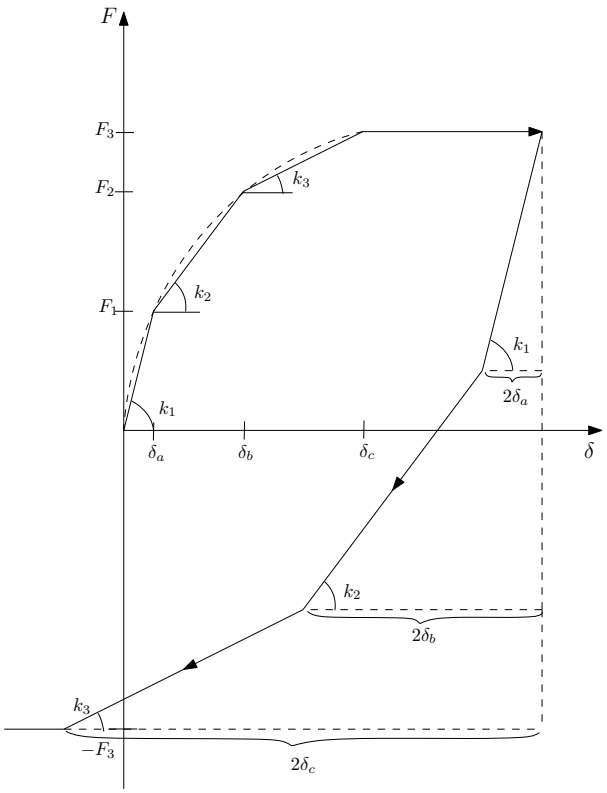

Figure 2. Unloading of nonlinear foundation.

This model was implemented in FAST v7 using 20 parallel springs, in order to obtain a smooth representation of the force-displacement relationship. The restrictions on these parameters were given by Equations (3) and (4).

Representation of nonlinear foundation response by a backbone curve has become common in dynamic soil-structure interaction studies. [28] have presented the results of dynamic analyses of an instrumented platform that verifies the use of this method. In that study, a similar method of representing foundation stiffness as presented in this paper has enabled capturing the change in the platform's natural period during heavy storms.

2.2.1. Values for the parameters of the backbone curve

For the target backbone curve representing the nonlinear relationship between load and displacement the hyperbolic function given in Equation (5) was selected. The parameters in this function are presented in Figure 3. The hyperbolic function was first suggested by [29], and has been shown to approximate the backbone curves resulting from loading of foundations to failure. Among others, [30] present one example of computed backbone curve for a platform foundation which approximately follows this function. It should be noted that the methodology presented in this paper is general and is independent of the selected function for the backbone curve. The hyperbolic function was chosen due to its simplicity and its common use by the geotechnical engineering community.

$$F = \frac{k_{max}\delta}{1 + \frac{k_{max}\delta}{F_{max}}} \tag{5}$$

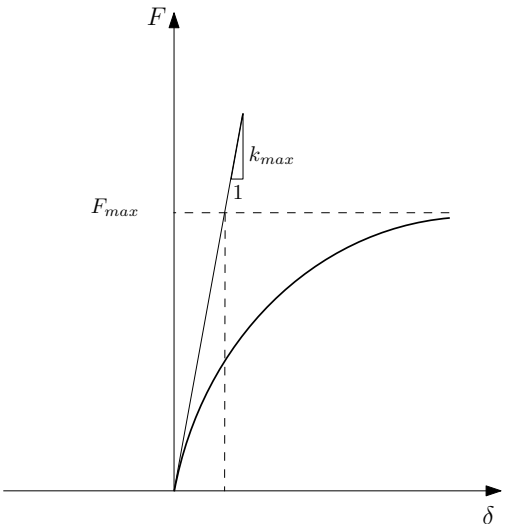

Figure 3. Hyperbolic backbone curve.

The initial stiffness k_{max} for each DOF, was taken from the stiffness matrix presented in Subsection 2.2.2 below. While for a given foundation one could establish the backbone curve by conventional geotechnical analyses or advanced finite element methods, a different approach was adopted in this paper for a more tuned sensitivity study. To this end, a simulation using the NREL 5MW with uncoupled springs at the bottom was made. Full-field wind and irregular waves were applied. The wind load was based on the IEC Kaimal turbulence model, using a wind speed at the hub height of the turbine of 12 m/s, and turbulence intensity $I_{ref} = 0.14$. Irregular waves were generated based on a JONSWAP spectrum. Significant wave height, H_s was set to 5 m and the peak spectral period T_p was set to 12 s. No current was applied. The simulation time was set to 630 s. The maximum moment caused by the loads was thereby found to be $M_{max,linear}$=109,000 kNm, omitting the first 30 s of the simulation to allow for a steady-state situation to occur. To create a realistic scenario, the maximum value of the backbone curve was set to M_{max}=5$M_{max,linear}$=545,000 kNm. Here, M_{max} corresponds to F_{max} in Figure 3 and δ is equivalent to the rocking, θ, of the spring. This assumption is motivated by the fact that foundations of wind turbines are designed to avoid large nonlinearity in the soil in order to prevent unacceptable permanent tilt of the tower. The factor of about 5 has been observed in several practical design to ensure acceptable margin against large nonlinear soil response. For simplicity, the nonlinear relationships were only considered for the two rotational DOFs and the translational springs were taken linear. The method presented here is general and can also include nonlinear horizontal response of the foundation. Therefore, this assumption does not represent any limitation of the presented methodology. This model is subsequently referred to as the *NL* (nonlinear) model. For a sensitivity study a reduced yield of M_{max}=3M_{max}=327,000 kNm was also considered. This case will be referred to as NL_{red} in the following text.

2.2.2. Initial foundation stiffness

The initial stiffness coefficients applied for the foundation stiffness matrix in this paper were based on a the soil-pile configuration considered by [19] and shown in Figure 4.

A simple Winkler model was used in [19] to compute the horizontal and rocking stiffness as listed in Equation (6).

$$\begin{bmatrix} \boldsymbol{k_{uu}} & \boldsymbol{k_{u\theta}} \\ \boldsymbol{k_{\theta u}} & \boldsymbol{k_{\theta\theta}} \end{bmatrix} = \begin{bmatrix} 2.57 \cdot 10^9 & 0.0 & 0.0 & -22.5 \cdot 10^9 \\ 0.0 & 2.57 \cdot 10^9 & 2.25 \cdot 10^{10} & 0.0 \\ 0.0 & 2.25 \cdot 10^{10} & 2.63 \cdot 10^{11} & 0.0 \\ -22.5 \cdot 10^9 & 0.0 & 0.0 & 2.63 \cdot 10^{11} \end{bmatrix} \tag{6}$$

The matrices $\boldsymbol{k_{uu}}$, $\boldsymbol{k_{u\theta}}$, $\boldsymbol{k_{\theta u}}$ and $\boldsymbol{k_{\theta\theta}}$ together considers the translational and rocking degrees of freedom in the two horizontal directions, and they have units $[N/m]$, $[N/rad]$, $[Nm/m]$ and $[Nm/rad]$, respectively.

DOI: 10.1002/we
Prepared using weauth.cls

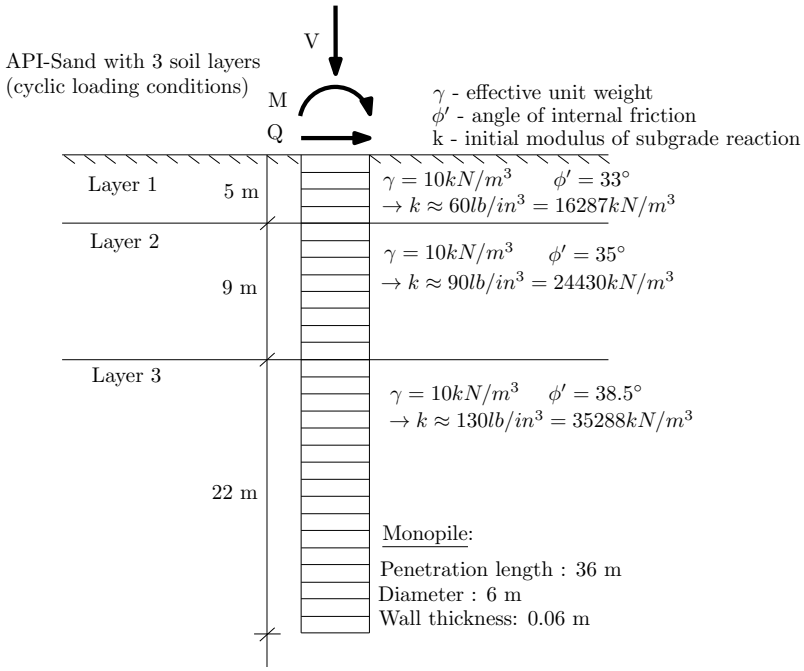

Figure 4. The soil profile from which the foundation stiffness matrix was derived [19].

While it is straightforward to treat the cross-coupling terms of the stiffness matrix (for example by use of a rigid link as described earlier), only the diagonal terms of the matrix in Equation (6) are used in the nonlinear analyses in the following sections.

In order to make an assessment of the stiffnesses computed by the Winkler model [19], the subgrade moduli, k, given for each layer in Figure 4 were converted to elastic moduli and used in the computational tool PILES [15] [16]. Figure 5 presents the variation of the real and imaginary parts of the computed rocking foundation impedance as functions of frequency.

The real part of the impedance gives variation of the stiffness with frequency, and the imaginary part represents the combined value of material and radiation damping of the foundation. According to this figure, the static rocking stiffness of the pile is equal to 1.93e11 Nm/rad which is about 35% lower than 2.63e11 computed by the Winkler model [19]. Figure 6 plots the variation of damping with frequency which starts with 0.5% at low frequencies and increases to 1.5% at 0.5 Hz.

The relatively large damping at higher frequencies, which cannot be computed by conventional Winkler models, could have considerable role in reducing the small-magnitude vibrations causing fatigue problems in the tower structure.

2.3. Implementation in FAST

FAST v7 possesses the option to implement a user-specified subroutine, *UserPtfmLd()*, for loads acting at the tower base. The loads applied by this subroutine are supposed to include contributions from external loads acting on the tower base other than those transferred from the wind turbine itself. Contributions from foundation stiffness could therefore be applied here.

NREL provides a dummy subroutine for implementation of linear springs at the base of the wind turbine model in FAST. This subroutine was used as a template for the new nonlinear foundation representation. In the NREL subroutine nonlinear springs in both lateral translational DOFs, and both rotational DOFs, are included. Because the response of OWTs is dominated by rocking, only the rocking springs are considered nonlinear. However, the procedure presented in this paper is general and can be equally applied to nonlinear translational springs.

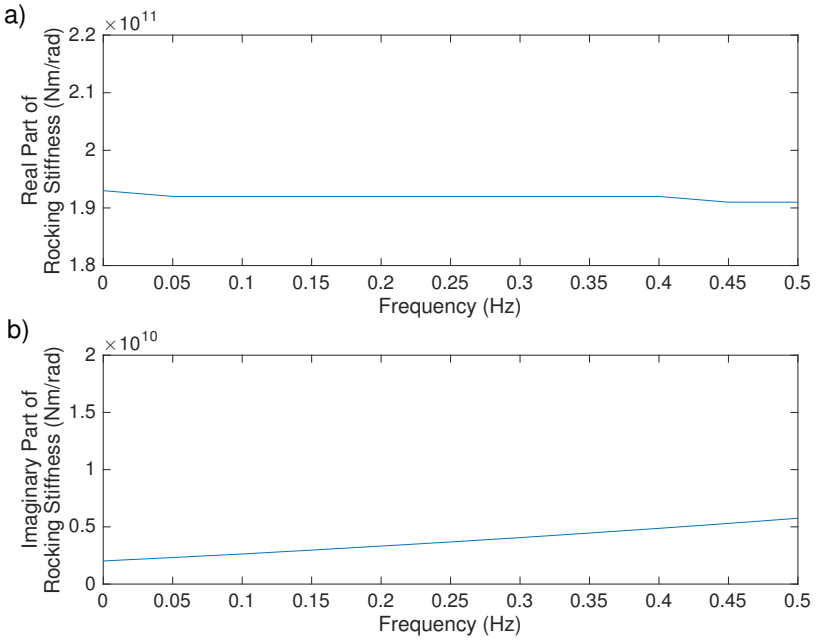

Figure 5. Real and imaginary parts of rocking foundation impedance as functions of frequency, computed in PILES[15][16].

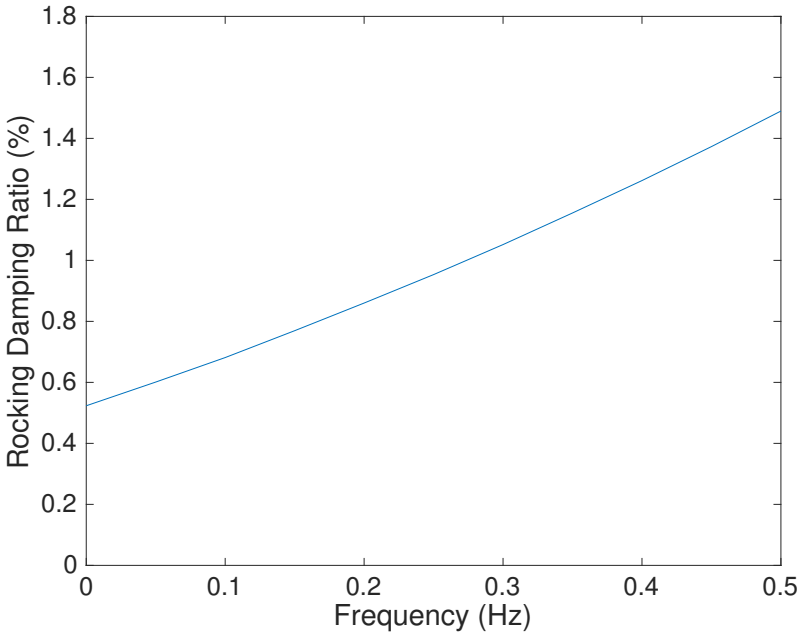

Figure 6. Damping as function of frequency computed in PILES [15][16].

It should be noted that FAST treats the foundation term as an external load calculated based on the previous displacement. This procedure is used in this study to implement a nonlinear foundation spring. [31] describes another procedure in which the complete system of equations are solved incrementally.

Also important to know is that mode shapes of the tower must be given as inputs to FAST. These should be obtained based on its boundary conditions, which include the foundation stiffness. For a nonlinear foundation, in theory the mode shapes of the tower should be updated for each new tangent stiffness of the foundation. For simplicity this has been ignored in the implementation, and in the following analyses, the mode shapes of the tower are based on the initial foundation stiffness.

2.3.1. FAST source code modification

As mentioned above, the subroutine *UserPtfmLd* was changed in this study to represent a nonlinear foundation in terms of parallel springs. The procedure applied is briefly presented here.

Structure of FAST FAST_Prog.f90 is the actual FAST Program. It opens and reads input files, sets up the initial values for all the DOFs, decides what analysis mode is to be run, runs it, and then ends the program. The program contacts the subroutine *TimeMarch*, which controls the execution of a typical time-marching simulation of the FAST code. This subroutine makes a call to a predictor-corrector subroutine, named *Solver*. After each call to Solver, an advancement in time is made. Then, all outputs are calculated in a following subroutine, *CalcOuts*, based on information from the Solver subroutine.

For the purpose of implementing foundation flexibility in FAST, Solver is the subroutine that is of interest. It solves the equations of motion by marching in time using a predictor-corrector scheme. So, for each time step, Solver estimates the next displacements and velocities in all DOFs through integration methods. These are fed into the subroutine *RtHS*, which calculates the equations of motion for a particular time step, and outputs a best estimate for the acceleration vector based on iterations. Among other subroutines, RtHS initiates *PtfmLoading*. This is the subroutine where the nonlinear foundation was implemented. Also, adjustments had to be made to Solver, and to the modules *Platform* and *RtHndSid*. Finally, the UserPtfmLd subroutine was introduced in the source file.

Subroutine UserPtfmLd For each of the 20 elastic perfectly-plastic springs, an uncoupled stiffness matrix and a yield force or -moment was defined.

In general the subroutine takes in forces and moments experienced by each of the springs in the last time step, together with previous and current estimates of displacements and velocities of the tower base. Using this information, the code estimates the current load in each of the elastic perfectly-plastic parallel springs, which is given as output from the subroutine.

Interaction between UserPtfmLd and remaining part of FAST Status of each of the springs are kept by means of loads in each spring, and displacements and velocities for the tower base from the previous time step. To manage this, the loads experienced by the springs are printed out from UserPtfmLd. These loads are saved in the Platform module, together with the total load on the tower base. The latter is the only output used by the rest of the program. After each time step, in Solver, these loads are renamed and stored in the RtHndSid module. This way, when the next time step is encountered, these forces are available for the next calculations.

3. RESULTS

3.1. Verification

To verify that the nonlinear foundation was appropriately implemented, the moment in the rocking springs was plotted against the corresponding rotation. To get a clear picture of the expected hysteresis curves, a harmonic wind load was used. Moreover, no waves were applied. The wind acts in the x-direction, therefore only the rotation of the tower about the y-axis is considered.

For a first visualization of the behavior of the foundation, a wind load that oscillates harmonically around zero was used. The values of the amplitude and period were set to mimic realistic behavior of wind. Periods of 30 s were applied, with velocity amplitudes ranging from 5 m/s to 10 m/s as illustrated in Figure 7.

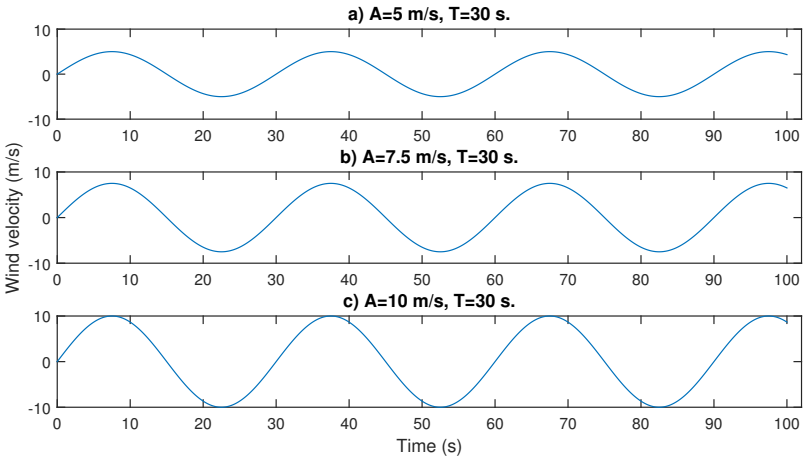

Figure 7. Harmonic wind loads.

Figures 8, 9 and 10 display plots of the hysteresis curves for the NL model with the harmonic loads shown in Figure 7a), b), and c), respectively. According to [3] wind turbines typically should not be allowed to tilt more than 0.5°. This calls for software that models the turbine behavior in the nonlinear regime correctly. For better comparison, the results in Figures 8, 9 and 10 are plotted together in Figure 11.The plots show clear differences in the hysteresis loops.

Wind Energ. 2010; **00**:1–29 © 2010 John Wiley & Sons, Ltd.
DOI: 10.1002/we
Prepared using weauth.cls

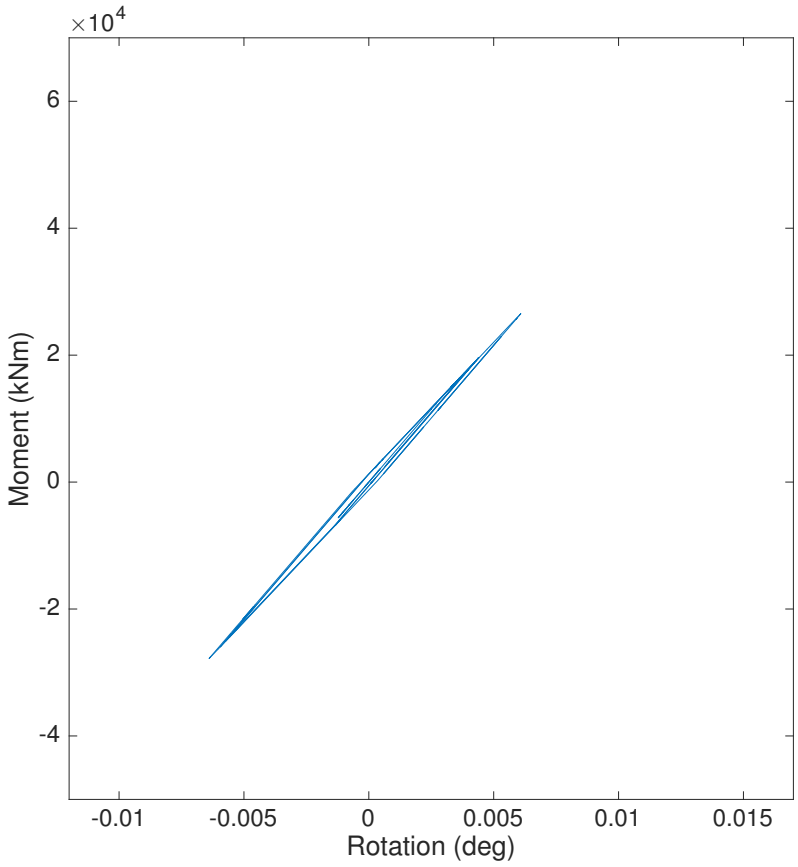

Figure 8. Hysteretic response for the NL model subjected to wind load in Figure 7 a).

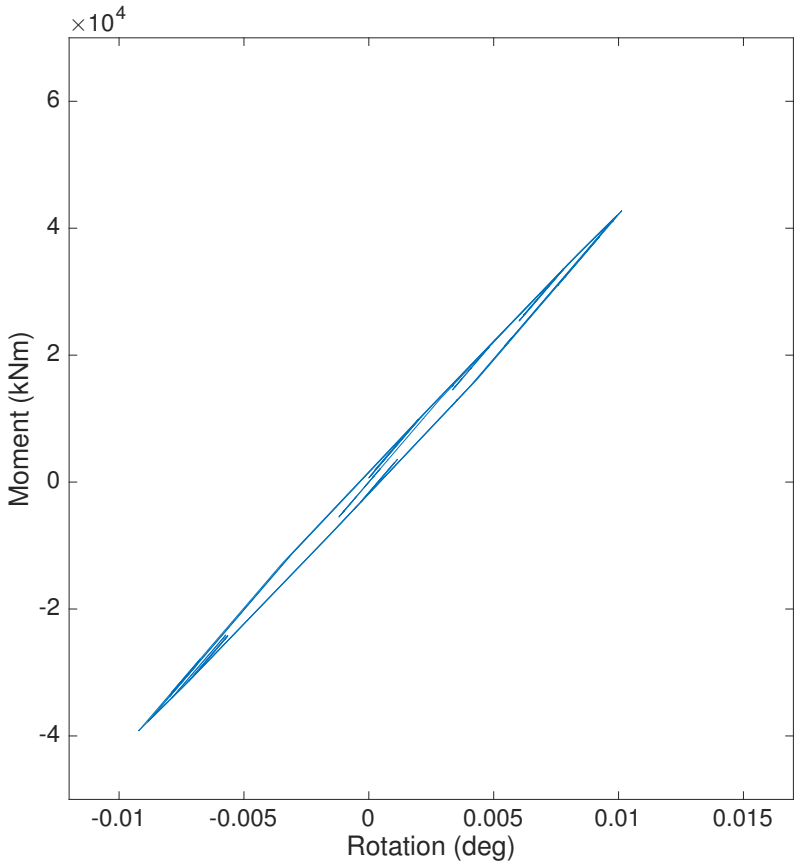

Figure 9. Hysteretic response for the NL model subjected to wind load in Figure 7 b).

Wind Energ. 2010; **00**:1–29 © 2010 John Wiley & Sons, Ltd.
DOI: 10.1002/we
Prepared using weauth.cls

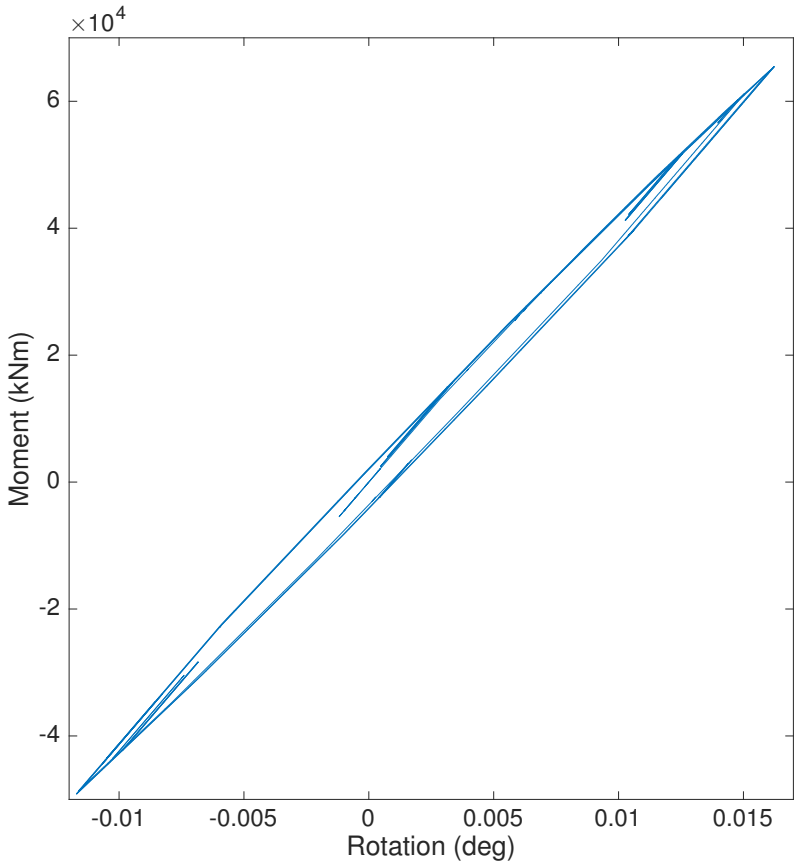

Figure 10. Hysteretic response for the NL model subjected to wind load in Figure 7 c).

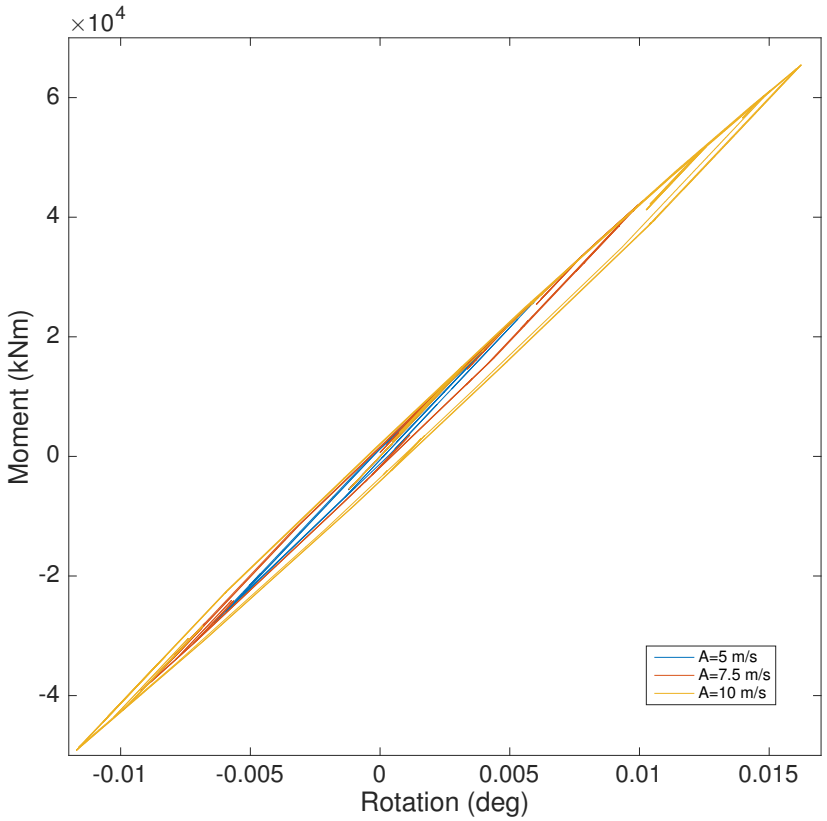

Figure 11. Combined plot of hysteretic response from Figures 8, 9 and 10.

Note that loads acting on the tower from the springs will be in the opposite direction of the movement of the tower. For visual simplicity, in the results in this section, the sign of the moment is changed.

The shape of the hysteresis curves clearly shows that a nonlinear behavior is successfully implemented. The area under the loop represents damping, as described in Section 1.1.

Wind Energ. 2010; **00**:1–29 © 2010 John Wiley & Sons, Ltd.
DOI: 10.1002/we
Prepared using weauth.cls

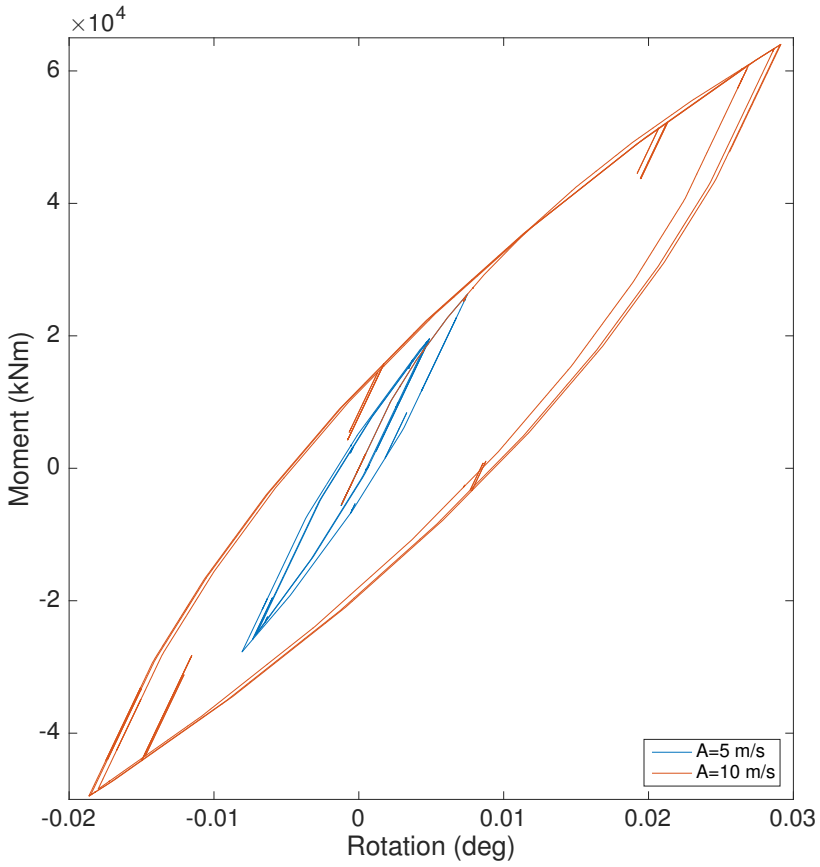

Figure 12. Hysteretic response for the NL_{red} model subjected to wind loads in Figures 7 a) and c).

The hysteresis curves for NL_{red} are plotted in Figure 12 for each of the wind loads in Figure 7. As revealed in this figure, NL_{red} exhibits a softer foundation behavior where nonlinearities are observed at smaller rotations. Correspondingly, the area under the hysteresis loop is larger, indicating more damping, as described in Section 1.1. The smaller loops nested in the large hysteresis loops, like the ones the red square in 12 marks, indicate partial unloading/reloading of the foundation spring at the tower's natural frequency. These small cycles have a stiffness corresponding to the initial stiffness of the moment-rotation curve, i.e. they are linear. Whereas the large cycles of the hysteresis represent the way the structure moves with the load, the smaller cycles enclosed are related to short period vibrations. While their amplitudes are small, they may be many, and thereby be significant to fatigue damage. The fact that these cycles are seen is yet another verification of the successful implementation of the soil model.

Figures 14, 15 and 16 display the results for loads with a period T=10 s for the NL model. This period is closer to the natural period of the turbine. As expected, the nonlinearities are more visible in the hysteresis curves plotted in these figures.

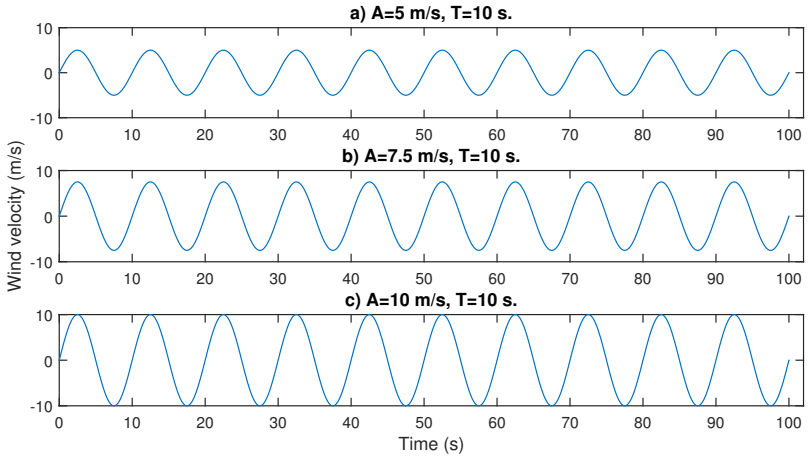

Figure 13. Harmonic wind loads.

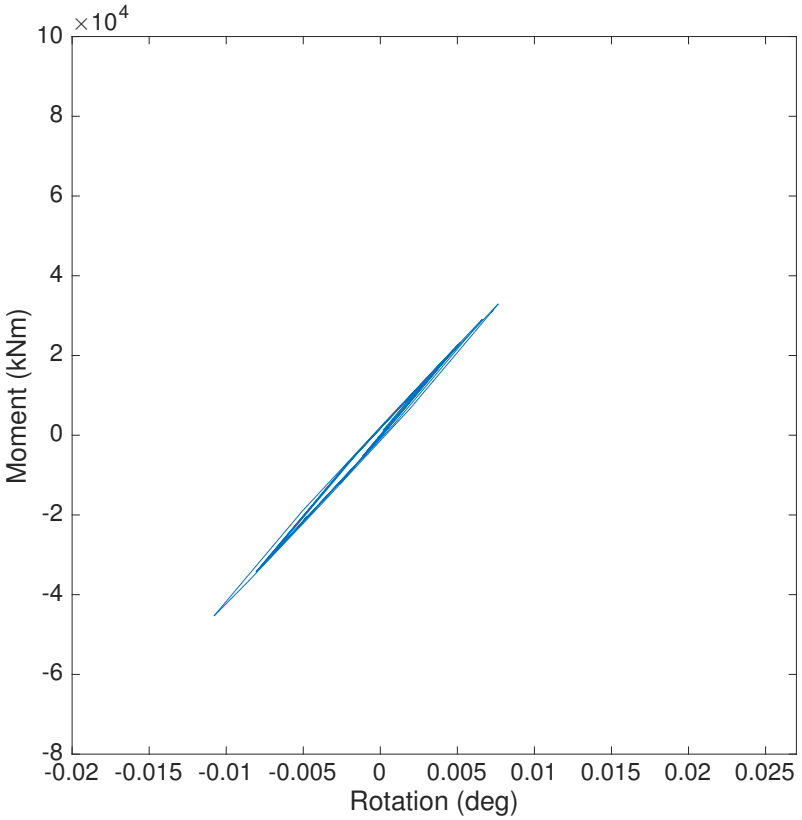

Figure 14. Hysteretic response for the NL model subjected to wind load in Figure 13 a).

Wind Energ. 2010; **00**:1–29 © 2010 John Wiley & Sons, Ltd.
DOI: 10.1002/we
Prepared using weauth.cls

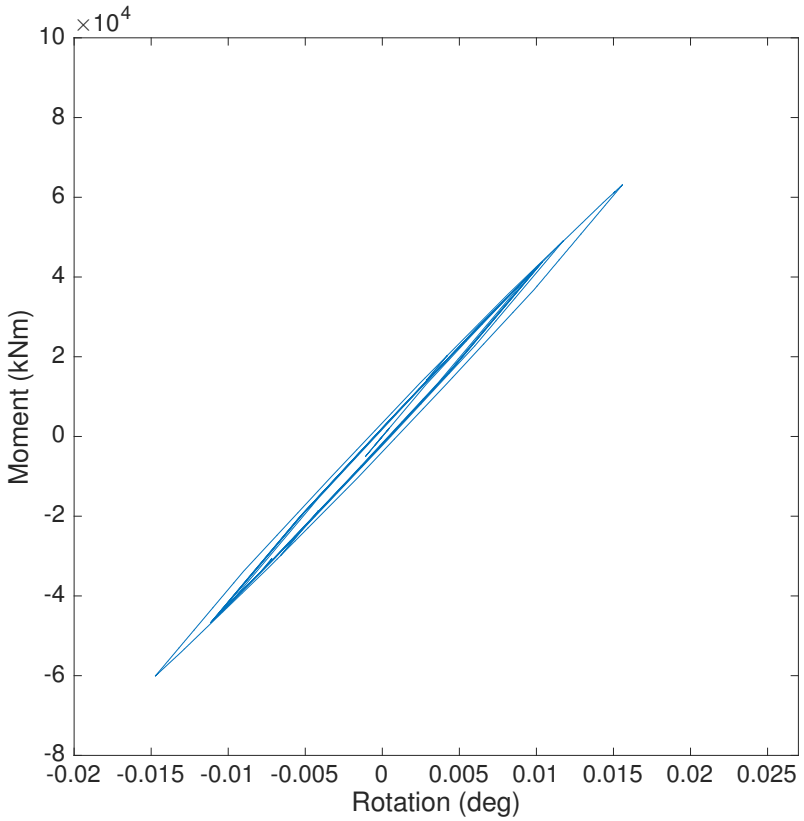

Figure 15. Hysteretic response for the NL model subjected to wind load in Figure 13 b).

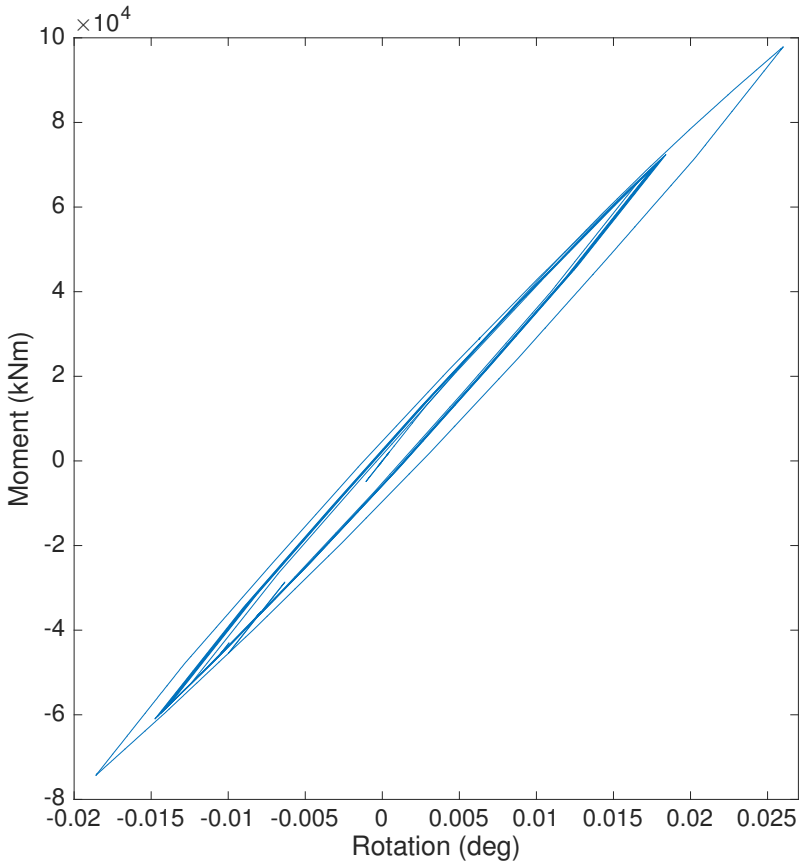

Figure 16. Hysteretic response for the NL model subjected to wind load in Figure 13 c).

In reality, the wind velocity oscillates around a mean wind speed of some value larger than zero. To obtain more realistic results while still being able to observe the hysteresis curves clearly, simulations were made for the NL model with harmonic wind having a mean velocity of 10 m/s, a period of 30 s and the same variety of amplitudes as considered previously (see Figure 17).

DOI: 10.1002/we
Prepared using weauth.cls

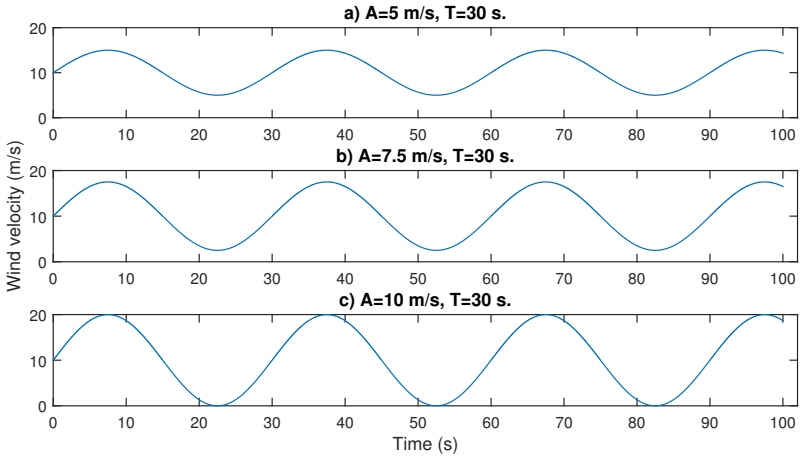

Figure 17. Harmonic wind loads. Mean velocity of 10 m/s.

Figures 18, 19 and 20 display the results of simulations for the loads in Figure 17. Due to the larger mean velocity in one direction, larger rotations are observed.

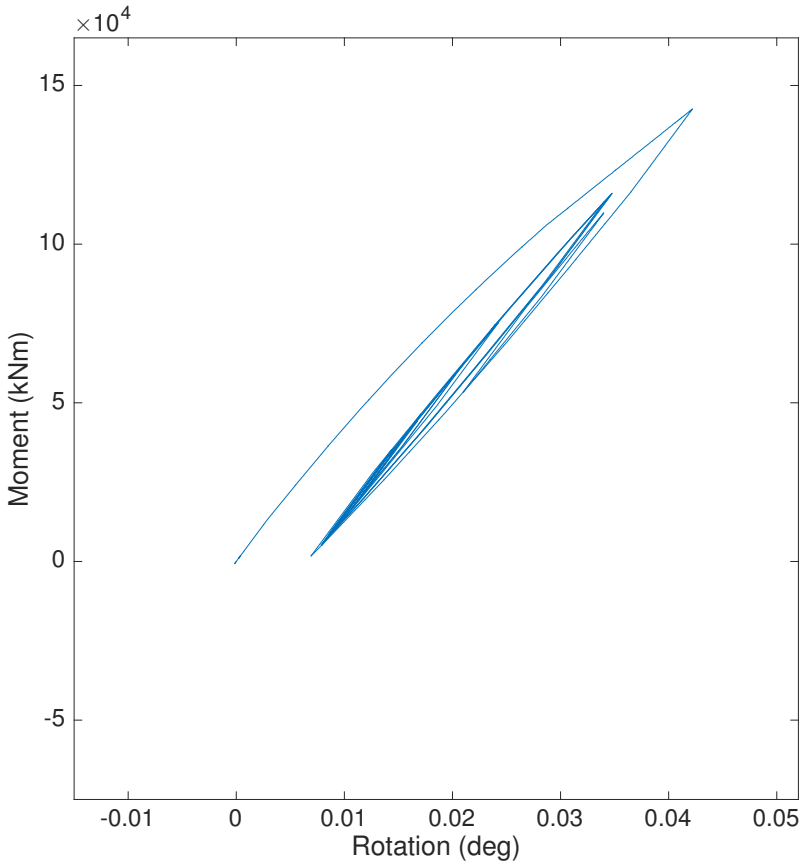

Figure 18. Hysteretic response for the NL model subjected to wind load in Figure 17 a).

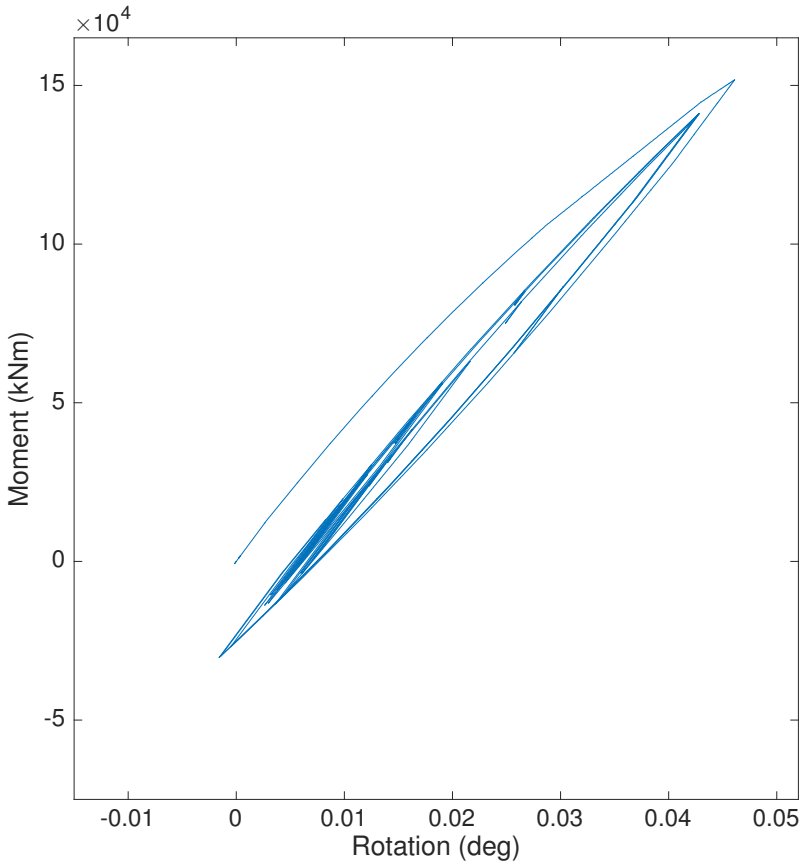

Figure 19. Hysteretic response for the NL model subjected to wind load in Figure 17 b).

Wind Energ. 2010; **00**:1–29 © 2010 John Wiley & Sons, Ltd.
DOI: 10.1002/we
Prepared using weauth.cls

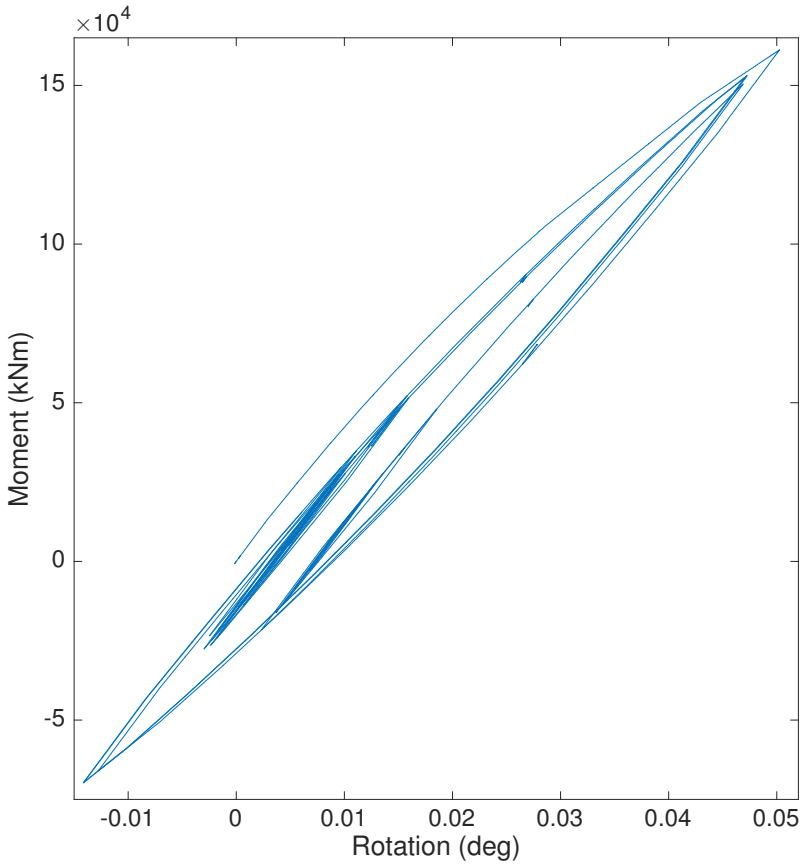

Figure 20. Hysteretic response for the NL model subjected to wind load in Figure 17 c).

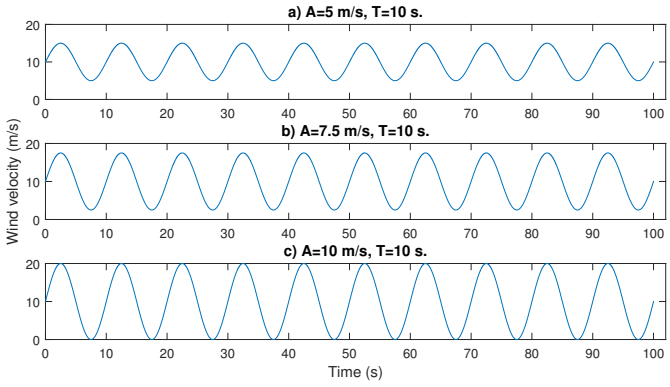

Figure 21. Harmonic wind loads. Mean velocity of 10 m/s.

To observe the effect of loading frequency for this loading condition, the simulations were repeated for a wind load with a period of 10 s as shown in Figure 21. The results are presented in Figures 22, 23 and 24. As expected, for a period of 10 s the rotations are even larger, due to the fact that the period of the load is closer to the natural periods of the turbine. Comparison of the plots in Figure 24 and 20 indicate a doubling of the tower rotation due to the change in the period of the load.

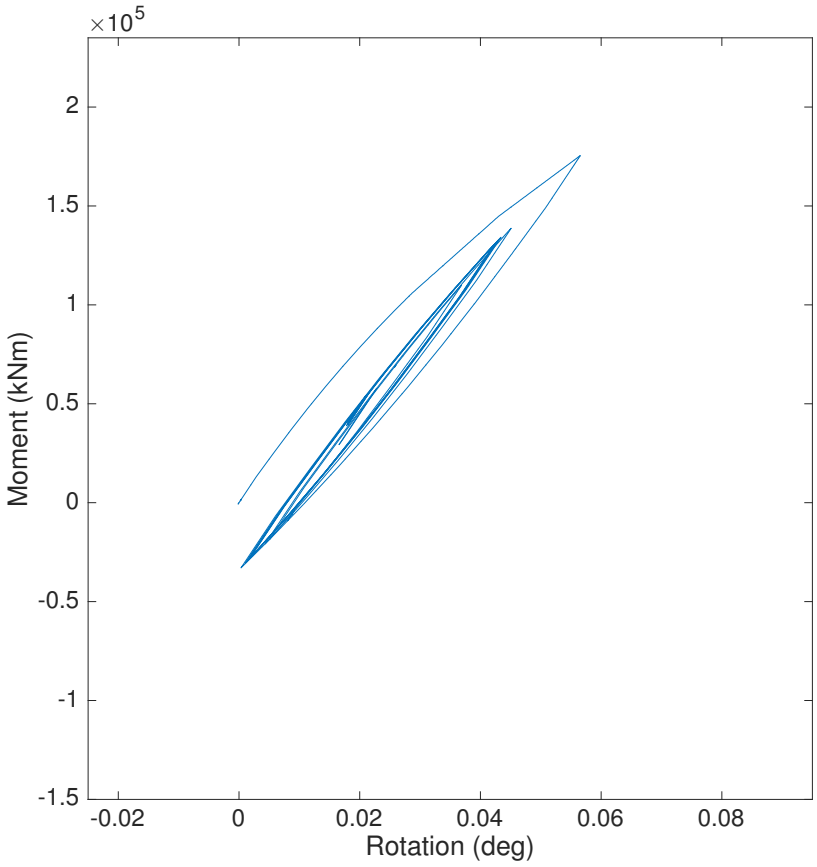

Figure 22. Hysteretic response for the NL model subjected to wind load in Figure 21 a).

Wind Energ. 2010; **00**:1–29 © 2010 John Wiley & Sons, Ltd.
DOI: 10.1002/we
Prepared using weauth.cls

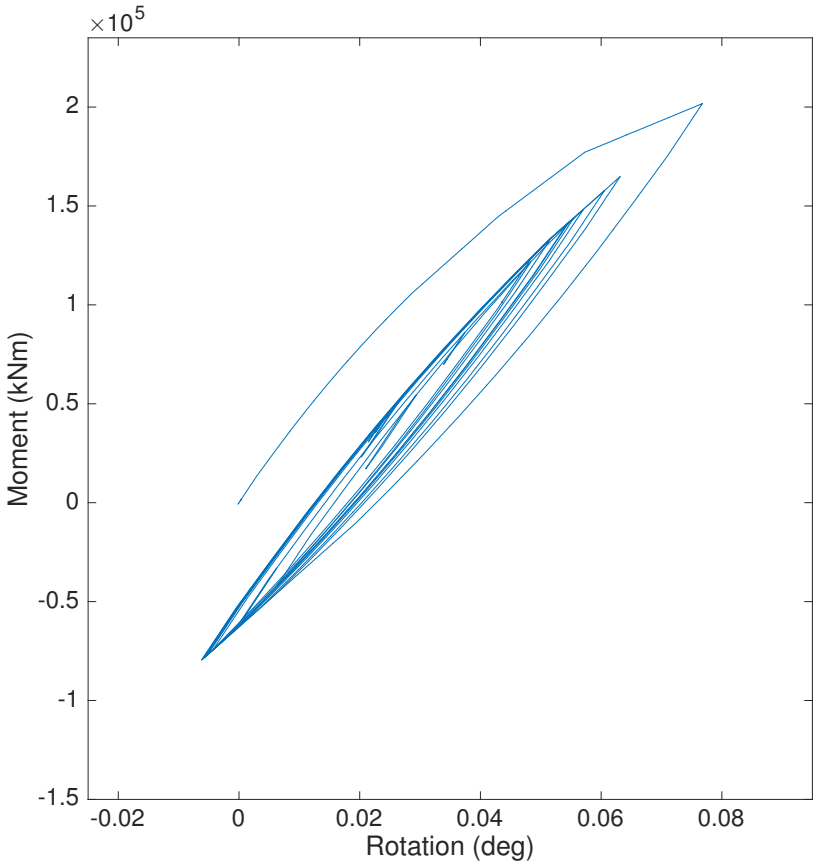

Figure 23. Hysteretic response for the NL model subjected to wind load in Figure 21 b).

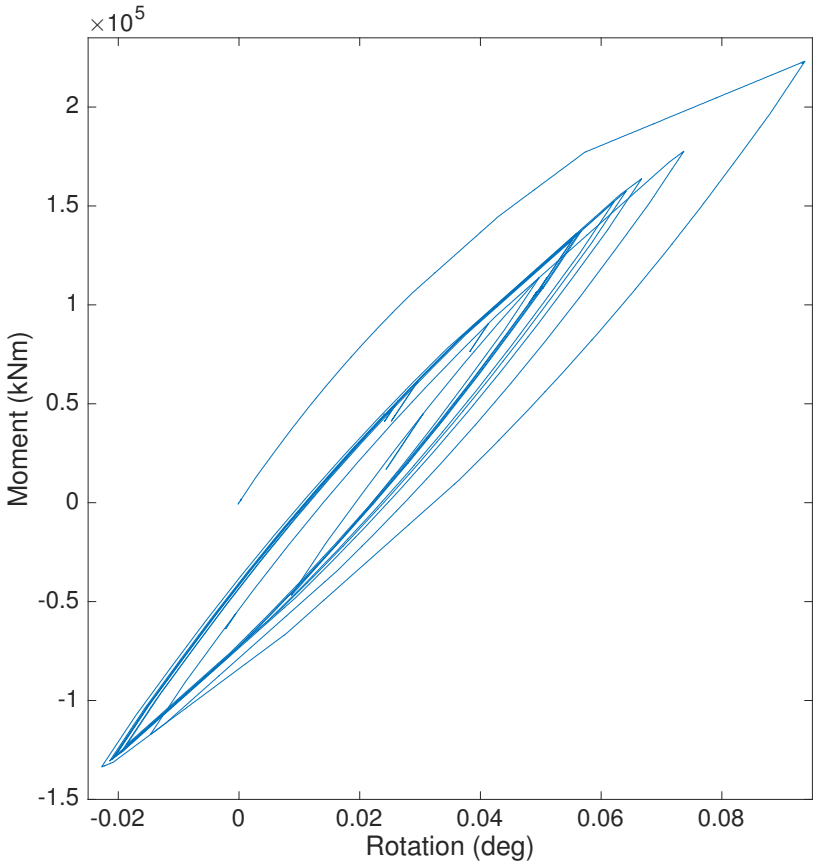

Figure 24. Hysteretic response for the NL model subjected to wind load in Figure 21 c).

3.2. Time Series of Response

For visualization, the time history of the response for the load case from Figure 17 c) was plotted.

Time series illustrating the rotation of the monopile at the mudline level is shown in Figure 25. Here, a comparison of the results from a model with uncoupled linear springs and from the nonlinear model can be seen. A small constant material damping has been included, hence the legend in the figure.

It is evident that the mudline rotation of the nonlinear model consequently lies above that of the linear one.

DOI: 10.1002/we
Prepared using weauth.cls

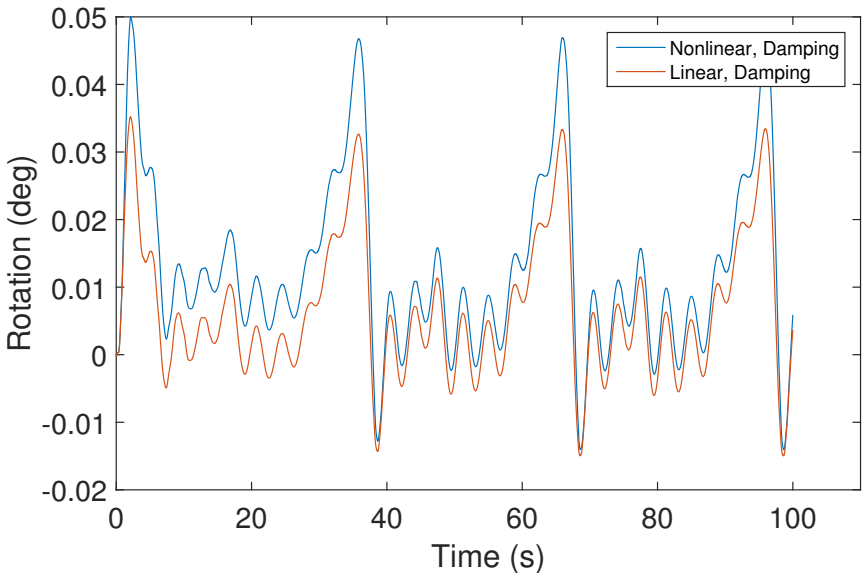

Figure 25. Rotation at the bottom of the monopile, i.e. at mudline level.

This result indicates that the nonliear model has a natural period that is larger, and therefore closer to the period of the wind.

4. DISCUSSION AND CONCLUDING REMARKS

The main objective of this paper has been to implement a nonlinear foundation representation in FAST v7. For this purpose, an OWT with a monopile support structure was considered, and the corresponding NREL 5MW reference turbine was used as a basis for the analyses. A nonlinear foundation was implemented in FAST v7 by means of the concept of parallel springs [6]. The performance of the model was demonstrated with the help of plots of moment vs rotation at the base of the monopile (i.e. mudline) for a number of loading conditions and foundations. To properly account for the cross-coupling of the horizontal and rocking stiffnesses, one should use a rigid link at mudline as described in Section 1.2. Moreover, for a more rigorous formulation, one needs to update the mode shapes of the tower for each new tangent stiffness of the foundation. These issues have been addressed in the paper and are straightforward to implement in FAST.

Some challenges that have not been regarded as scope, should be given awareness. For each time step, the stiffness matrix of the foundation should be included in the overall stiffness matrix of the complete wind turbine system. Currently, influence of the foundation on the support structure is merely applied as an external force, disregarding the fact that the soil-pile interaction should be considered as a part of whole turbine system. This requires an extensive change in the source code of FAST. Moreover, the rigid link described in Section 1.2 should be applied for uncoupled stiffness matrices so that their response equals that of a coupled stiffness matrix. Also, as mentioned previously, the mode shapes of the tower should be updated for each new tangent stiffness of the foundation.

ACKNOWLEDGEMENT

This paper is based partly on the first author's Master's thesis at the Department of Structural Engineering, Norwegian University of Science and Technology (NTNU). The second author acknowledges partial support from the project

”Reducing cost of offshore wind by integrated structural and geotechnical design (REDWIN)” funded by the Norwegian Research Council, grant number 243984. The authors would like to thank Dr. Jason Jonkman for advice on the structure of FAST for code development.

REFERENCES

1. RenewableUK. Offshore wind 2015. URL http://www.renewableuk.com/en/renewable-energy/wind-energy/offshore-wind/\index.cfm.
2. Association TEWE. The european offshore wind industry - key trends and statistics 2014. *Report*, The European Wind Energy Association 2014. URL http://www.ewea.org/fileadmin/files/library/publications/statistics/EWEA-\European-Offshore-Statistics-2014.pdf.
3. Lombardi D, Bhattacharya S, Muir Wood D. Dynamic soilstructure interaction of monopile supported wind turbines in cohesive soil. *Soil Dynamics and Earthquake Engineering* 2013; **49**(0):165–180, doi:http://dx.doi.org/10.1016/j.soildyn.2013.01.015. URL http://www.sciencedirect.com/science/article/pii/S0267726113000171.
4. Passon P, Kühn M. State-of-the-art and development needs of simulation codes for offshore wind turbines 2005. URL http://www.ieawind.org/task_23/Subtask_2S_docs/Meeting%2004_Roskilde%20II/Risoe%\202005-State_of_the_art.pdf.
5. Jonkman J, Butterfield S, Musial W, Scott G. Definition of a 5-mw reference wind turbine for offshore system development. *Report*, National Renewable Energy Laboratory 2009.
6. Iwan WD. On a class of models for the yielding behavior of continuous and composite systems. *Journal of Applied Mechanics* 1967; **34**(3):612–617, doi:10.1115/1.3607751. URL http://dx.doi.org/10.1115/1.3607751, 10.1115/1.3607751.
7. Damgaard M, Andersen LV, Ibsen LB, Andersen J. Time-varying dynamic properties of offshore wind turbines evaluated by modal testing 2013.
8. Schløer S. Fatigue and extreme wave loads on bottom fixed offshore wind turbines - effects from fully nonlinear wave forcing on the structural dynamics. Phd thesis 2013.
9. Meyer V. Overview of offshore wind turbine foundation research at ngi 2015; URL http://www.ngi.no/upload/77442/03-OWT%20Foundation%20Research%20at%20NGI_vme.pdf.
10. Tarp-Johansen NJ, Andersen L, Christensen E, Mørch C, Frandsen S. Comparing sources of damping of cross-wind motion 2009. URL http://proceedings.ewea.org/offshore2009/allfiles2/406_EOW2009presentation.pdf.
11. Jonkman W J; Musial. Offshore code comparison collaboration (oc3) for iea task 23 offshore wind technology and deployment. *Report*, National Renewable Energy Laboratory (NREL) 2010.
12. Damgaard M. Dynamic properties of offshore wind turbine foundations. Phd thesis 2014.
13. Novak M. Dynamic stiffness and damping of piles. *Canadian Geotechnical Journal* 1974; **11**(4):574–598.
14. Damgaard M, Andersen L, Ibsen LB. Assessment of dynamic substructuring of a wind turbined foundation applicable for aeroelastic simulations. *Wind Energy* 2014; **18**(8):1387–1401.
15. Kaynia AM, Kausel E. Dynamics of piles and pile groups in layered soil media. *Soil Dynamics and Earthquake Engineering* 1991; **10**(8):386–401.
16. Kaynia AM. Piles, chapter 7. *Boundary element techniques in geomechanics* 1993; :209–241.
17. Bush E, Manuel L. *Foundation models for offshore wind turbines*. Aerospace Sciences Meetings, American Institute of Aeronautics and Astronautics, 2009, doi:doi:10.2514/6.2009-103710.2514/6.2009-1037. URL http://dx.doi.org/10.2514/6.2009-1037, doi:10.2514/6.2009-1037.

18. American Petroleum Institute. Recommended practice 2a-wsd planning, designing, and constructing fixed offshore platforms - working stress design. *Report* 2014.
19. Passon P. Memorandum: Derivation and description of the soil-pile-interaction models. *Report*, University of Stuttgart 2006.
20. Jonkman J, Butterfield S, Passon P, Larsen T. Offshore code comparison collaboration within iea wind annex xxiii: Phase ii results regarding monopile foundation modeling 2007.
21. Hededal O, Klinkvort RT. A new elasto-plastic spring element for cyclic loading of piles using the p-y-curve concept. *Numerical Methods in Geothecincal Engineering*, vol. 1, Taylor and Francis Group, 2010; 883–888.
22. Klinkvort RT. Centrifuge modelling of drained lateral pile-soile response. Phd thesis 2012.
23. Castellano A. Developent and implementation of a frictional 3d soil model for aero-elastic computations of offshore wind turbines. Msc thesis 2014.
24. Schløer S, Castellano A, Bredmose H. Impementation of a hysteretic 3d soil model in an aeroelastic code. dynamic analysis of an offshore wind turbine in misaligned wind and waves 2015.
25. Carswell W, Johansson J, Løvholt F, Arwade SR, Madshus C, DeGroot DJ, Myers AT. Foundation damping and the dynamics of offshore wind turbine monopiles. *Renewable Energy* 2015; **80**(0):724–736, doi:http://dx.doi.org/10.1016/j.renene.2015.02.058. URL http://www.sciencedirect.com/science/article/pii/S0960148115001743.
26. Krathe VL. Aero-hydro dynamic analysis of offshore wind turbine - implementation of nonlinear soil-structure interaction in software fast. Msc thesis 2015.
27. Jonkman J. Personal communication 2015.
28. Kaynia AM, Norn-Cosgriff K, Andersen KH, Tuen KA. Nonlinear foundation spring and calibration using measured dynamic response of structure 2015.
29. Duncan JM, Chang CY. Nonlinear analysis of stress and strain in soils. *Journal of the Soil Mechanics and Foundations Division, ASCE* 1970; **96**(SM5):1629–1653.
30. Kaynia AM, Andersen KH. Development of nonlinear foundation springs for dynamic analysis of platforms. *Proc. Frontiers in Offshore Geotechnics III, ISFOG*, Meyer (ed.), Taylor Francis; 1067–1072.
31. Chopra AK. *Dynamics of Structures*. 4th edn., Prentice Hall: University of California, Berkely, 2011.